Contents list available at Journal of e-Science Letters

Journal of e-Science Letters

journal homepage: http://scienceletters.researchfloor.org/

Synthesis and Characterization of Photovoltaic Properties of Tin Based Lead-Free Perovskite Solar Cell

Aloke Verma[1,*], Arun Kumar Diwakar[2], Tripti Richhariya[1], Avinash Singh[1] and Ekta Chandrawanshi[1]

[1]Department of Physics, Kalinga University, Naya Raipur, 492101 (CG) India
[2]Government Model Residential Girls College, Kondagoan 494226 (CG) India

ARTICLE INFO

Article History:
Received 29 June 2022
Revised 12 September 2022
Accepted 13 September 2022
Available Online 14 September 2022

Keywords:
SnF2,
Perovskite solar cell (PSCs),
Film preparation,
ITO, Thin Film,
Vacuum vapor deposition (VVDs),
Lead Free Perovskite (LFPs)

ABSTRACT

While conversion efficiency is continually improving, PSCs are also making strides toward commercialization. However, its structure contains Pb, a hazardous material, which contradicts the original aim of solar cells to save energy and protect the environment and impedes their commercialization. The goal of this article is to increase the device performance of lead-free tin-based PSCs, which are environmentally beneficial. In this research, SnF2 is initially precipitated in perovskite solution and employed as a heterogeneous nucleation site, which aids tin-based perovskite precipitation and growth into a flat and compact film following annealing. The lattice contraction of perovskite becomes increasingly visible as x increases, and the size of the unit cell of the film surface grows greater. The goal of this work is to x increase from 0 to 0.5, the performance of the device's environmentally-friendly lead-free tin-based PSCs is 2.1% and VOC = 0.35 V when x = 0.5. In this research, SnF2 is initially precipitated in perovskite solution and employed as a heterogeneous nucleation site, allowing tin-based perovskite to precipitate quicker and more evenly, and then develop into a flat and compact film after annealing. As x increases, the lattice shrinkage of perovskite becomes more visible, and the unit cell size of the film surface grows bigger.

1. Introduction

The current evolution shows us with hard facts that our future growth will rely more on green and natural renewable energy, in addition to the production and exploitation of renewable energy. Solar photovoltaic power generation is the most promising of these because of its simple concept, modular structure, simple operation and maintenance of generator sets, and fast building duration. The entire unit may be erected on desert terrain or on building roofs, which is the only approach to best, generate and utilize solar energy approx 3.0% to 27% (Meng et. al. 2020).
LFPs materials are now a popular research trend in the perovskite sector, and tin-based perovskite, as the principal alternative for lead, has attracted widespread attention (Meng et al.' 2020; Verma et al., 2019). Despite the fact that tin-based perovskite has a wide absorption bandwidth and carrier mobility is too high, in addition to being environmentally friendly, the instability of SnF_2 in the air severely limits the increase of PCEs of its solar devices (Verma et al., 2019).

As a result, the purpose of this thesis is to investigate the effect of preparation technology and materials on the performance of tin-based PSCs. With the $FASnI_3$ tin-based PSCs as the fundamental device, different concentrations of SnF_2 were put into the perovskite solution, and the excellence of film formation was enhanced by utilizing SnF_2 to improve the PCEs of the cell.
The one-step solution approach is now
the most widely used method for creating tin-based perovskite thin films. Because it has been shown that the preparation process is highly

*Corresponding Author: Aloke Verma
E-mail Address: alokeverma1785@gmail.com
DOI: http://dx.doi.org/10.46890/SL.2022.v03i03.003

significant for the performance of PSCs, this research has chosen to investigate the effect of the preparation method and materials on the performance of tin-based PSCs (Heo et al., 2018). The $FASnI_3$ tin-based PSCs is used as the basic device in present work to deeply understand the role of SnF_2 in assisting film formation, and it is expounded for the first time that SnF_2 is the mixed nucleation point, and the method of single crystal growth is creatively used to prove that SnF_2 can effectively improve the nucleation rate, which can be operated outside the glove box, and it is simple, easy, and highly (Aftab et al., 2021).

2. Preparation method

The PCEs of PSCs is heavily influenced by the perovskite film's quality. Light absorption efficiency, charge transfer efficiency, and carrier diffusion length all have a strong influence on the excellence of perovskite thin films (Verma et al., 2021). At the moment, the design of perovskite films is primarily separated into two methods: liquid phase and gas-phase. The liquid phase approach consists of three steps: one-step spin coating, step-by-step infiltration, and two-step spin coating (Li et al., 2020).

The one-step solution method is the simplest preparation method, with the following rough process: first, perovskite base is mixed and dissolved in appropriate solvents in proportion, which are generally polar aprotic solvents such as N, N dimethylformamide, dimethyl sulfoxide, γ-butyrolactone, and so on (Ke et al., 2019).

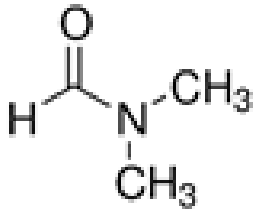

N, N dimethylformamide

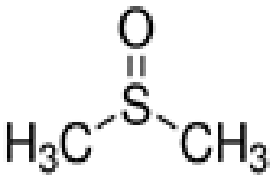

dimethyl sulfoxide

γ-butyrolactone

After fully stirring until the solution is clear, it is directly spin-coated on the substrate, and then the solvent is removed by thermal annealing. At this time, the precursor will be assembled into perovskite (Verma et al., 2019; Li et al., 2020; Ke et al., 2019).

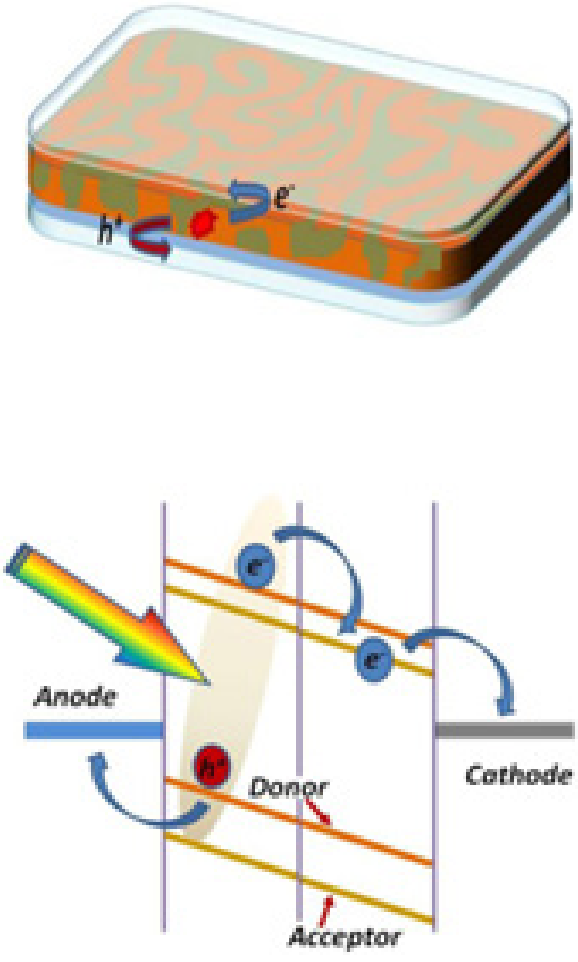

Fig. 1. The functioning concept of a perovskite battery is depicted schematically.

Solvent engineering is a popular approach for creating Pb-based perovskite batteries. The typical preparation procedure is depicted in Fig. 2 (Verma et al., 2019; Heo et al., 2018).

GBL/DMSO, DMF/DMSO, GBL/NMP, and other mixed solvents are often used to make perovskite precursors. Rinsing the antisolvent during spin coating necessitates the antisolvent's compatibility with perovskite precursor solvents, but it does not dissolve perovskites such as toluene, chlorobenzene, and ether (Verma et al., 2020).

With anti-solvent dripping, all soluble components in the precursor will become uniform perovskite crystallites and the adduct of MI_2, delaying the quick reaction between FAI/MAI and SnI_2, and assisting in the formation of very uniform and compact films (Verma et al., 2019; Sho et al., 2021).

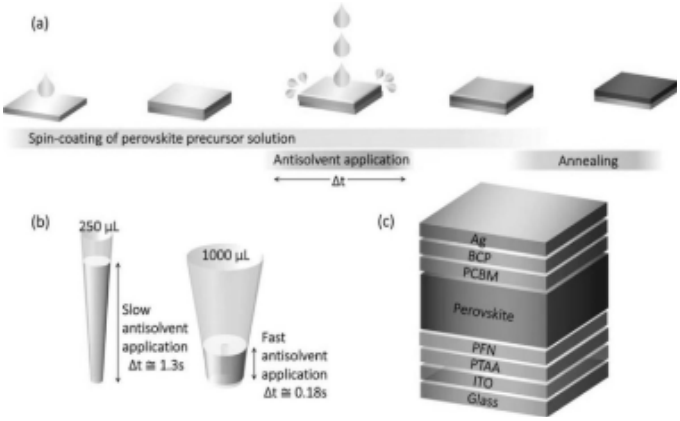

Fig. 2. Diagram of the solvent engineering approach for producing perovskite thin films.

Vacuum vapor deposition is used to create the perovskite film. The fundamental procedure is as follows: the perovskite precursors are put in various evaporation sources, the chamber is sealed and vacuumed to a specific degree, and the evaporation source is heated to allow the materials within to evaporate (Ke et al., 2019; Verma et al., 2020). Basically, the path of mean free of molecules expands in a high vacuum, and these molecules leave the evaporation source and deposit on the top substrate.

Already reported by various researchers, $MAPbI_3$ films were produced by vacuum vapor deposition using $PbCl_2$ with MAI double source evaporation. A planar heterojunction arrangement yielded a 15.4 percent energy conversion efficiency, as illustrated in Fig. 3 (Verma et al., 2019; Li et al., 2020).

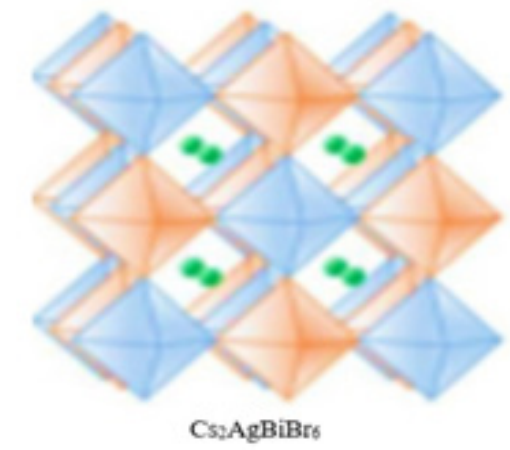

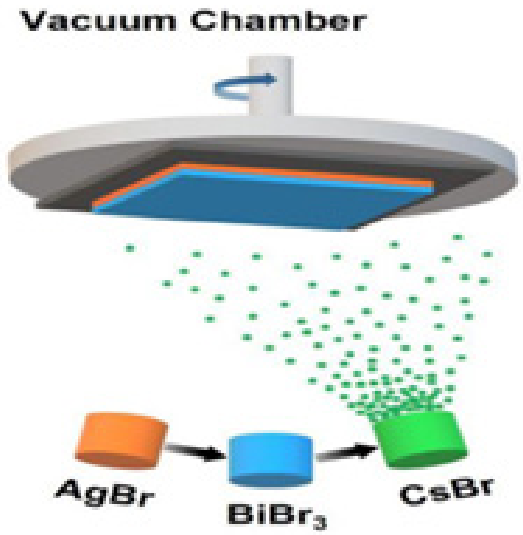

Fig. 3. Dual-source evaporation vapor deposition was used to produce perovskite thin films.

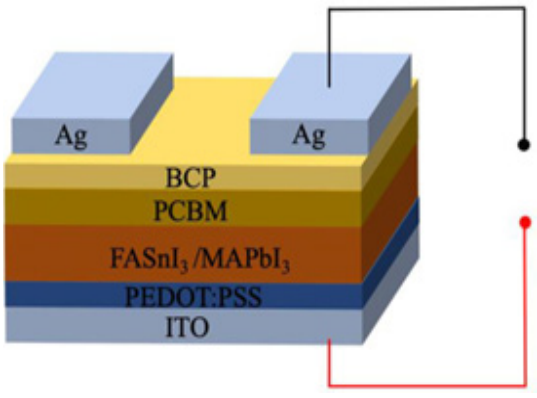

Fig. 4. The device structure of tin-based PSCs.

To completely achieve high-quality perovskite films, the co-evaporation technique with two or more sources must tightly regulate the evaporation rate of each component to ensure the precise proportion of reactants. Requirements of the necessity for a high temperature and high vacuum environment, equipment conditions are high, and the overall cost is high, making large-scale manufacturing in the future impossible (Verma et al., 2021).

3. Research method

The crystallization rate of tin-based perovskite batteries is excessively quick during the film production process, resulting in inadequate film coverage and significant roughness. The effect on device performance is mostly seen by low short-circuit current and a low filling factor. Furthermore, the water–oxygen stability of tin-based perovskite batteries is quite low, which not only complicates experimentation and characterization but is also detrimental to commercial development (Varadwaj et al., 2018).

According to several study findings, there are numerous advantages of doping polymer into perovskite thin films. For starters, long-chain polymers aid in the formation of networks between perovskite grains and can significantly enhance the morphology of thin films (Verma et al., 2020).

Second, due to the cross-linking action of the polymer, the dehumidification process is considerably hindered, resulting in more uniform perovskite grains. Third, some research has found that perovskite doped with polymer has a reduced density of trap states because the polymer efficiently passivates the surface of the perovskite particles (Verma et al., 2019; Verma et al., 2020). Fourth, the polymer aggregates between grains, acting as a bridge for charge transfer; last, the hydrophobic polymer packed at the grain border of perovskite can increase perovskite stability.

The following are the experiments and supplies used to all material of Sigma Aldrich in ITO conductive glass, PEDOT:PSS aqueous solution, $CH(NH_2)_2I$(FAI), $CH(NH_2)_2Br$(FABr), SnI_2, SnF_2, N, N dimethylformamide (DMF), dimethyl sulfoxide (DMSO), PCBM, chlorobenzene, BCP, Ag particles The day before device preparation, the tin-based perovskite base solution is normally finished Verma et al., 2021; Verma et al., 2020).

370 mg of SnI_2, 170 mg of FAI, and 15 mg of SnF_2 (molar ratio: 1:1:0.1) are weighed and put in a reagent bottle in a glove box with a nitrogen environment. Add 790 µL DMF and 210 µL DMSO (volume ratio: 4:1) and stir at room temperature with a magnetic stirrer. The yellow translucent $FASnI_3$ perovskite base solution is getting when the solution is cleared (Sho et al., 2021).

When the spin-coating perovskite light-absorbing layer's base solution is pure $MASnIBr_2$ solution without additive, the obtained perovskite film is observed under SEM, and it can be seen that there are many randomly distributed large grains with different thicknesses and surface roughness, and they are not always connected, resulting in the exposure of large porous layers (Verma et al., 2019; Varadwaj et al., 2018).

According to this, after adding SnF_2, SnF_2 precipitates first with the volatilization of solvent in the spin coating process and uniformly distributes across the substrate as heterogeneous nucleation spots, facilitating the quicker and more uniform precipitation of $MASnIBr_2$ (Verma et al., 2022).

In contrast to the chaotic and rapid precipitation of tin-based perovskites in the absence of SnF_2, the precipitation length and pace of $MASnIBr_2$ are more consistent following the addition of SnF_2, allowing smooth and dense large grains to develop throughout the annealing process. In contrast to the chaotic and fast precipitation of tin-based perovskites without SnF_2, the precipitation length and pace of $MASnIBr_2$ are more consistent after adding SnF_2, allowing smooth and dense large grains to be produced by Oswald ripening throughout the annealing phase (Verma et al., 2019; Verma et al., 2022).

The trans-p-i-n structure is employed in the device and the perovskite battery structure is as follows from bottom to top: ITO/PEDOT:PSS/$(FA)_{1-y}(MA)_ySnBr_xI_{3-x}$/PCBM/BCP/Ag, ITO substrate cleaning, transmission layer preparation, and buffer layer and electrode evaporation Fig. 4 depicts the device's structural diagram (Verma et al., 2020). Solixon A-20 was used to measure the J–V characteristic curve and sunshine simulator.

The scanning voltage range is 1V to 20V, and the battery's effective area is 2×2 cm. The X-ray diffractometer is frequently used to characterize the structure, phase, crystallization degree, crystal orientation, and other properties of crystal samples (Ke et al., 2019). When an X-ray impacts on a crystal, the lattice vibration causes electrons to radiate electromagnetic waves into space, and this electromagnetic wave leads electrons of surrounding atoms to emit electromagnetic waves into space again. Analytical Tech. Ltd. SEM3069 X-ray diffractometer is used in present work. The bombardment target is made of copper and has a wavelength of 0.154 nm (Verma et al., 2021).

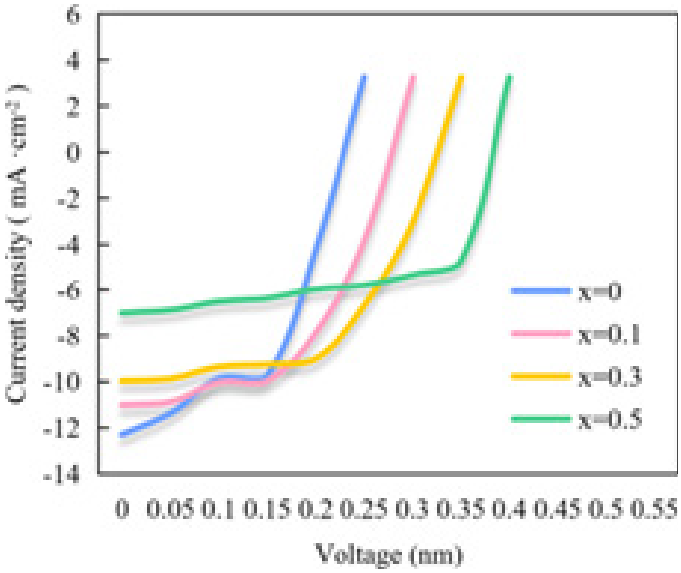

Fig. 5. J–V curves of PSCs devices with different x.

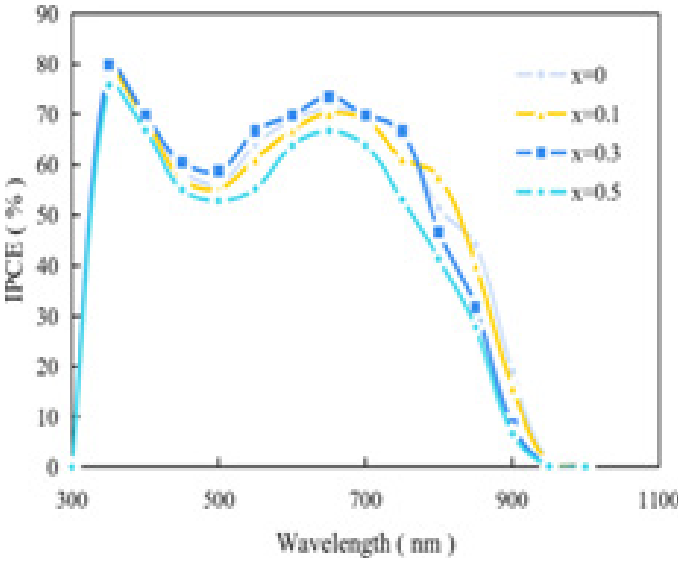

Fig. 6. IPCE curve.

The Hall effect tester is frequently used to assess the electrical characteristics of semiconductor materials such as carrier concentration, mobility, and resistivity. It is mostly tested using the Hall effect theory (Li et al., 2020). The Hall effect occurs when charged particles are deflected by Lorentz force in a magnetic field, resulting in a new transverse extra electric field perpendicular to the electric and magnetic fields (Ke et al., 2019). The charge build-up will stay balanced when the transverse electric field force provided to the carriers equals Lorentz's force (Verma et al., 2021).

4. Results and discussion

The I element in $FASnI_3$ was largely replaced by Br ions in this section, and thin films and battery devices with $FASnBr_xI_{3-x}$ perovskite as absorption layer were created, where *x* is the mole number of Br ions doped (Verma et al., 2019; Verma et al. 2021). This section investigates the device performance, crystallization, surface morphology, and light-trapping capabilities of *x* (= 0, 0.1, 0.3, 0.5). Figures 5 and 6 show J–V curves and IPCE diagrams of perovskite battery devices with varying x values. These figures show that when the doping concentration of Br ions increases, the PCE of the devices increases, as represented mostly in V_{OC} and FF, while the short-circuit current decreases (Verma et al., 2020).

With *x* = 0.5, the device efficiency reaches 1.803% and V_{OC} is 0.3283 V. The IPCE curve in Fig. 6 is consistent with the J–V curve, and when x is changed, the edge of the IPCE curve exhibits a blue shift phenomenon, demonstrating that the doping concentration of Br may regulate the perovskite bandgap (Verma et al., 2019; Varadwaj et al., 2018).

The XRD pattern of perovskite thin films doped with Br ions in various amounts is shown in Fig. 7, and perovskite thin films are deposited on PEDOT:PSS thin films (Verma et al., 2021). When compared to $FASnI_3$ films, the films doped with Br have higher crystallinity. Enlarging the angle of the major peak in Fig. 7(a) leads in Fig. 7(b), where it was discovered that when bromine doping concentration increases, the position of the film's primary diffraction peak changes to a bigger angle (Li et al., 2020).

Because the radius of Br ions is smaller than that of I ions, it is thought that this transformation phenomenon, which shows that some Br ions with smaller ionic radii can be successfully doped

into the crystal structure of perovskite to replace I ions, changes the crystal structure of $FASnI_3$ films to some extent and causes the perovskite lattice to contract (Verma et al., 2020).

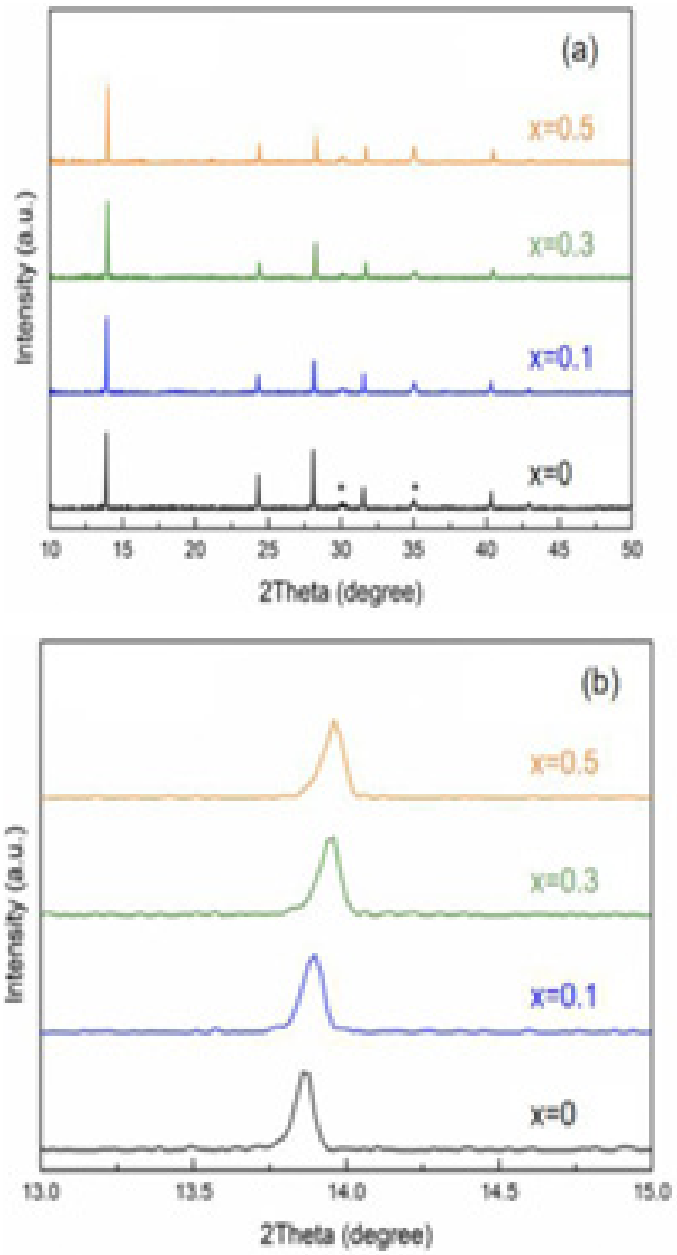

Fig. 7. XRD diagrams of perovskite thin films with different *x*.

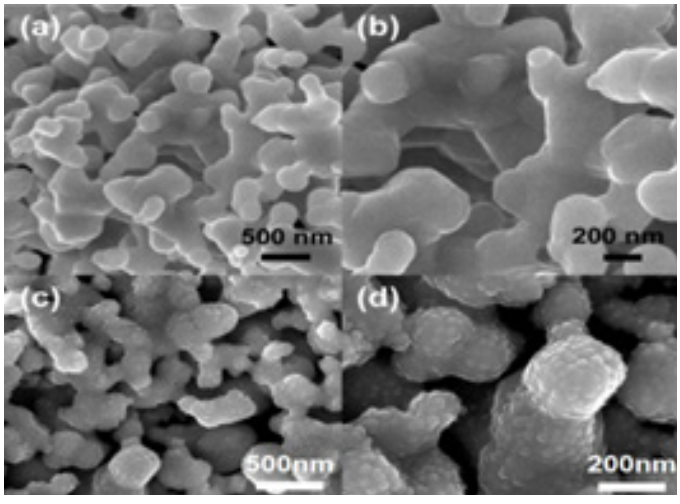

Fig. 8. SEM images of perovskite thin films corresponding to different *x*.

SEM images of perovskite thin films with varied concentrations of Br ions were studied to better understand the impact of the doping concentration of Br on the surface morphology of the thin films. The tested thin films were deposited on PEDOT: PSS thin films, and were annealed at 80°C for 15 min with diethyl ether as an anti-solvent. As shown in Fig. 8 (Verma et al. 2019; Verma et al., 2021; Verma et al., 2020).

As shown in Fig. 8, the perovskite crystal grains are polyhedral, and the cell size of the perovskite film corresponding to different doping concentrations has no discernible change, whereas the surface of undoped perovskite crystal cells has striations, whereas the surface of doped perovskite crystal cells is smoother and more complete. Under the four conditions, the film texture is uniform and the unit cells are closely arranged, a small amount of white material is precipitated in the corresponding film at $x = 0.5$, and the film quality is high on the whole (Verma et al., 2020).

5. Conclusion

PSCs, a novel form of the thin-film solar cell, offers several advantages, including easy processing, high conversion efficiency, rate of conversion, and adaptability. However, high-performance perovskite cells currently all include harmful heavy metal lead, limiting its wide-scale applicability and commercialization. There is currently no effective solution to the problem that Sn^{2+} in tin-based perovskite is easily oxidized. To isolate oxygen as much as possible, spin coating preparation of tin-based perovskite active layer must be performed in an inert gas glove box, which is also not suitable for industrial large-scale manufacturing.

References

1. X. Meng, Y. Wang, J. Lin, X. Liu, X. He, J. Barbaud, T. Wu, T. Noda, X. Yang, L. Han.Joule, 4(4):902-12 (2020).

2. A. Verma, A. K. Diwakar, R. P. Patel. Int. J of Sci. Research in Physics and Applied Sciences, 7(2):24-6 (2019).

3. J. H. Heo, J. Kim, H. Kim, S. H. Moon, S. H.Im, K. H. Hong. The journal of physical chemistry letters,

9(20):6024-31 (2018).

4. A. Aftab, M. I. Ahmad. Solar Energy, 216:26-47 (2021).

5. A. Verma, A. K. Diwakar, R. P. Patel, P. Goswami. InAIP Conference Proceedings, 2369(1) p.020006 (2021).

6. M. Li, W. W.Zuo, Y. G. Yang, M. H.Aldamasy, Q. Wang, S. H. Cruz, S. L. Feng, M.Saliba, Z. K. Wang, A. Abate. ACS Energy Letters, 5(6):1923-9 2020).

7. W. Ke, M. G. Kanatzidis. Nature communications, 10(1):1-4 (2019).

8. A. Verma, A. K. Diwakar, P. Goswami, R. P. Patel, S. C. Das, A. Verma. Solid State Technology, 63(6):13008-11 (2020).

9. S. Shao, M.Nijenhuis, J. Dong, S.Kahmann, H. Gert, G.Portale, M. A.Loi. Journal of Materials Chemistry A, 9(16):10095-103 (2021).

10. A. Verma, A. K. Diwakar andR. P. Patel. InEmerging Materials and Advanced Designs for Wearable Antennas 2021 (pp. 149-153) (2021).

11. A. Varadwaj, P. R.Varadwaj, K. Yamashita. ChemSusChem 2018 Jan 23;11(2):449-63 (2018).

12. A. Verma, A. K. Diwakar, T. Richhariya, A. Singh,L. Chaware. Journal of Optoelectronics Laser, 41(6), pp.230-233 (2022).